-Supporting Information-

Photoelectrochemical Bioanalysis Platform of Gold Nanoparticles Equipped Perovskite Bi_4NbO_8Cl

Yi-Fan Ruan,[†] Nan Zhang,[†] Yuan-Cheng Zhu,[†] Wei-Wei Zhao,[,†,‡] Jing-Juan Xu[*,†] and Hong-Yuan Chen[†]*

[†]State Key Laboratory of Analytical Chemistry for Life Science and Collaborative Innovation Center of Chemistry for Life Science, School of Chemistry and Chemical Engineering, Nanjing University, Nanjing 210023, China

[‡]Department of Materials Science and Engineering, Stanford University, Stanford, California 94305, United States

* E-mail: zww@nju.edu.cn; zww@stanford.edu Fax: +86-25-89684862; Tel: +86-25-89684862

* E-mail: xujj@nju.edu.cn; Fax: +86-25-89687294; Tel: +86-25-89687294

This material includes the XRD spectra of synthetic source Bi_2O_3, BiOCl, Nb_2O_5, prepared Bi_4NbO_8Cl and standard spectrum of Bi_4NbO_8Cl (Figure S1), XPS spectra of Bi_4NbO_8Cl and Au modified ITO electrode (Figure S2), EDX spectroscopy of Au NPs/ Bi_4NbO_8Cl/ITO electrode (Figure S3), CV curves (Figure S4-S6) and PEC GSH detection based on Au NPs/Bi_4NbO_8Cl electrodes (Figure S7-S8).

XRD, EDX, and XPS Characterizations.

Figure S1 depict the XRD spectra of Bi_2O_3, BiOCl, Nb_2O_5, prepared Bi_4NbO_8Cl and standard spectrum of Bi_4NbO_8Cl (ICSD#93487) (PDF#54−0818), respectively. Synthetic sources are separated in the XRD patterns with synthetic Bi_4NbO_8Cl. XRD pattern of synthetic Bi_4NbO_8Cl is also determined. The result revealed the formation of Bi_4NbO_8Cl and also the presence of impurities,[1] as compared to the standard substance of Bi_4NbO_8Cl (ICSD#93487) (PDF#54−0818).

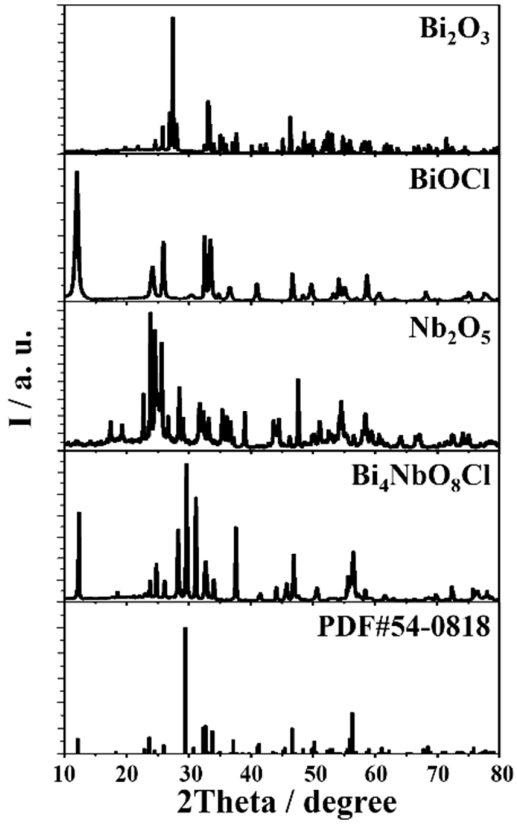

Figure S1 XRD pattern of synthetic source Bi_2O_3, BiOCl, Nb_2O_5, prepared Bi_4NbO_8Cl and standard substance of Bi_4NbO_8Cl (ICSD#93487) (PDF#54−0818).

The EDX spectroscopy of Au NPs/Bi_4NbO_8Cl/ITO electrode was obtained as shown in Figure S2, Au peak was observed in the spectroscopy.

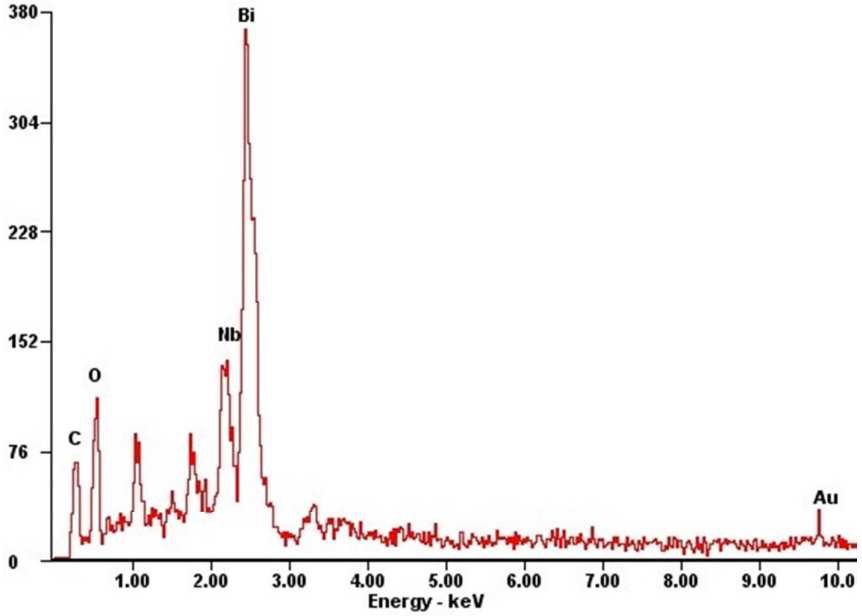

Figure S2 EDX Spectroscopy of Au NPs/Bi_4NbO_8Cl /ITO electrode.

The XPS spectra of (A) Bi_4NbO_8Cl and (B) bare Au NPs on the substrate were recorded as shown in Figure S3.

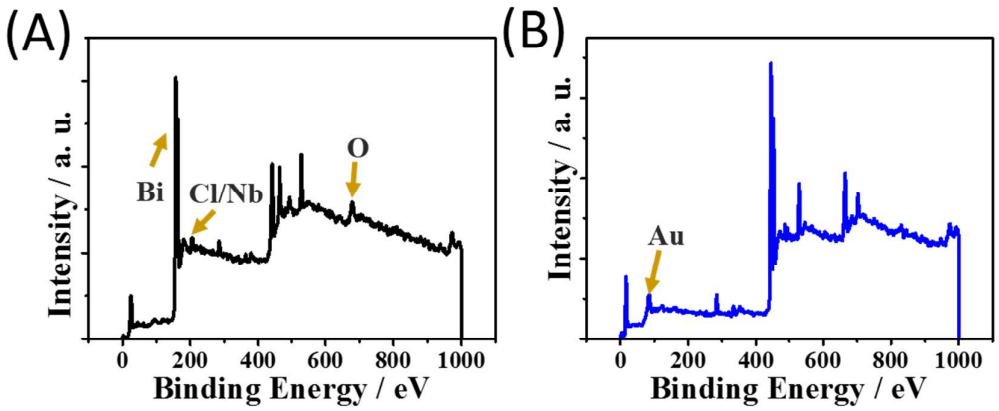

Figure S3 XPS spectra of (A) Bi_4NbO_8Cl and (B) Au NPs modified ITO electrode.

Electrochemical Characterizations.

The electrochemical properties were then studied through cyclic voltammogram (CV) using the traditional three-electrode system consisting a working electrode of ITO, Bi_4NbO_8Cl/ITO, Au NPs/ITO or Au NPs/Bi_4NbO_8Cl/ITO electrode, a counter electrode of Pt wire, and an Ag/AgCl reference electrode. As shown in Figure S4 A, no obvious peaks appears within the CV of bare ITO, while the CV of Bi_4NbO_8Cl/ITO in Figure S4 B showed an oxidation peak at ca. −0.2 V, which was attributed to the surface oxidation of perovskite from Bi(III) to higher valence state, and a similar peak around −0.2V was observed in CV of Bi_2O_3/ITO as shown in Figure S5. Figure S5 demonstrated the CV of the Au NPs/ITO, the oxidation peak at near 1.0 V was caused by the oxidization of Au NPs, while the cathodic peaks at 0.5 V and ca. −0.4 V should be attributed to the reductions of gold oxide.[2,3] Figure S4 C displayed the CV of the Au NPs/Bi_4NbO_8Cl/ITO, with the magnified curve in the range of 0.0 − 1.0 V shown in Figure S4 D. In comparison, the CV of Au NPs/Bi_4NbO_8Cl/ITO (Figure S4 C) comprised both the oxidation and reduction peaks appeared in the Bi_4NbO_8Cl/ITO (Figure S4 B) and Au NPs/ITO (Figure S6), indicating the integration of Au NPs with perovskite on the ITO electrode.

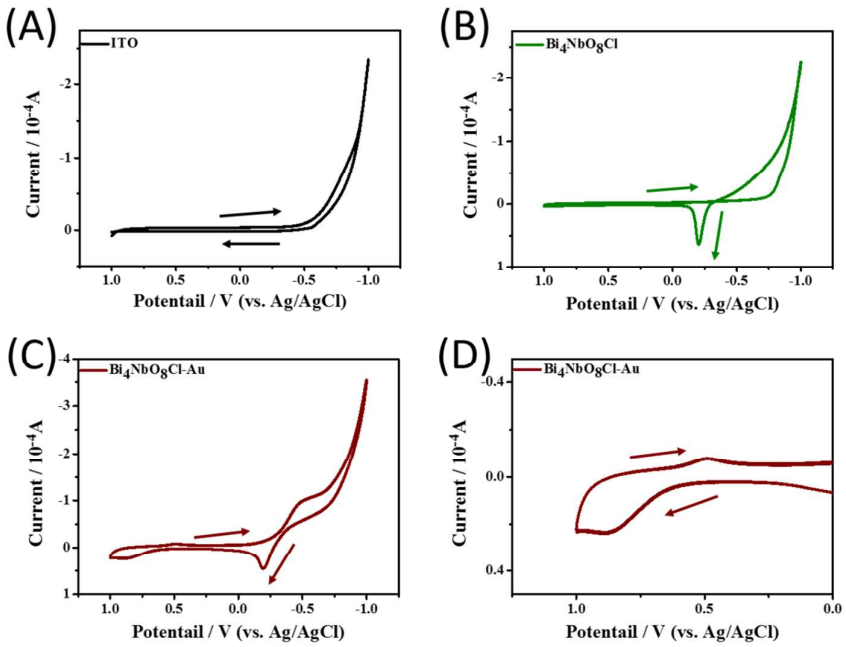

Figure S4 CV curves of (A) ITO, (B) Bi_4NbO_8Cl/ITO, (C) Au NPs/Bi_4NbO_8Cl/ITO, and (D) a partial enlarged view of Au NPs/Bi_4NbO_8Cl/ITO. The experiments were performed in 0.1 mol L^{-1} PBS containing 1.0% sodium citrate (mass fraction, 0.034 mol L^{-1}) under nitrogen with scan rate of 0.1 V/s.

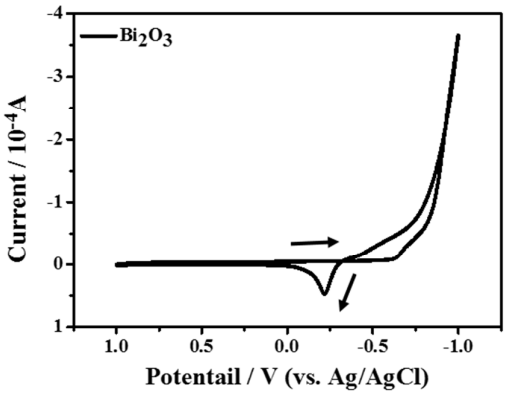

Figure S5 CV curves of Bi_2O_3/ITO. The experiments were performed in 0.1 mol L^{-1} PBS containing 1.0% sodium citrate (mass fraction, 0.034 mol L^{-1}) under nitrogen with scan rate of 0.1 V/s.

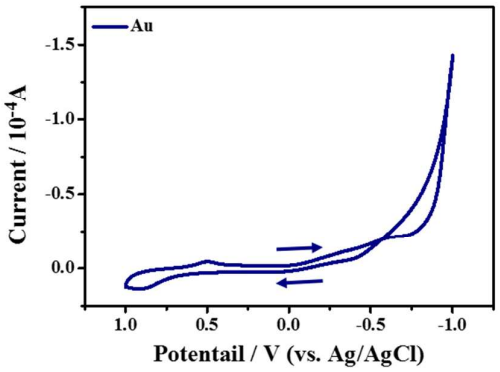

Figure S6 CV curves of Au NPs/ITO. The experiments were performed in 0.1 mol L^{-1} PBS containing 1.0% sodium citrate (mass fraction, 0.034 mol L^{-1}) under nitrogen with scan rate of 0.1 V/s.

PEC GSH Detection

In addition, GSH as another important biomolecule was detected with the results shown in Figure S7 and S8. Effect of different GSH concentrations on the differential photocurrent responses against the bare Bi_4NbO_8Cl and Au NPs/Bi_4NbO_8Cl electrodes were then investigated with the results shown in Figure S8 A and B, respectively. The progressive photocurrent responses of the two electrodes were then further compared, and the specific working dependence and the corresponding linearity regions were depicted in Figure S8 C and D.

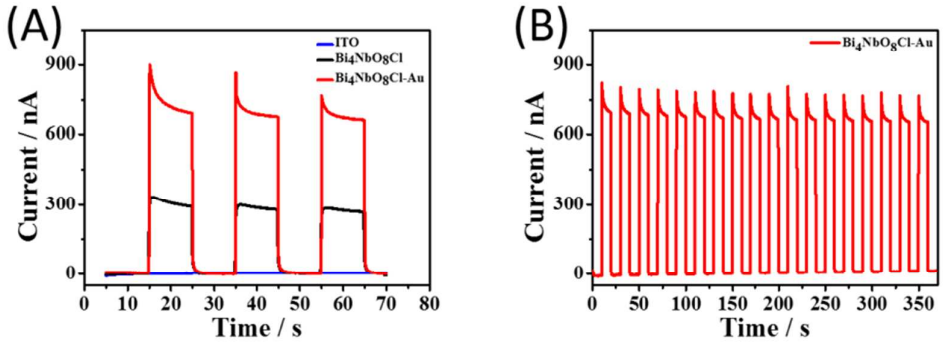

Figure S7. (A) Photoresponses of ITO electrode (blue), Bi_4NbO_8Cl (black) and Au NPs/Bi_4NbO_8Cl (red) for detection of 0.05 mol L^{-1} GSH. (B) Stability of the Au NPs/Bi_4NbO_8Cl in the detection of 0.05 mol L^{-1} GSH

Effect of different GSH concentrations on the differential photocurrent responses against the bare Bi_4NbO_8Cl and Au NPs/Bi_4NbO_8Cl electrodes were then investigated with the results shown in Figure 4A and B, respectively. We further compared the progressive photocurrent responses of the two electrodes, and the specific working dependence and the corresponding linearity regions were depicted in Figure 4C and D. The detection limits of bare Bi_4NbO_8Cl and Au NPs/Bi_4NbO_8Cl were 10^{-6} mol L^{-1} and 10^{-7} mol L^{-1}, respectively, with the corresponding linearity regions of 5×10^{-3} mol L^{-1} – 5×10^{-2} mol L^{-1} and 5×10^{-4} mol L^{-1} – 5×10^{-2} mol L^{-1}, respectively.

The precision and reproducibility of this PEC bioassay was evaluated by relative standard deviation (RSD). Analyzed from the experimental results, the RSD of 6.9% was obtained by measuring the same 0.01 mol L^{-1} sample with at least four electrodes prepared independently at the identical experimental conditions. Besides, after several repeated measurements, no significant difference of photocurrent response could be

observed as compared to the result obtained, indicating the stable readout for signal collection.

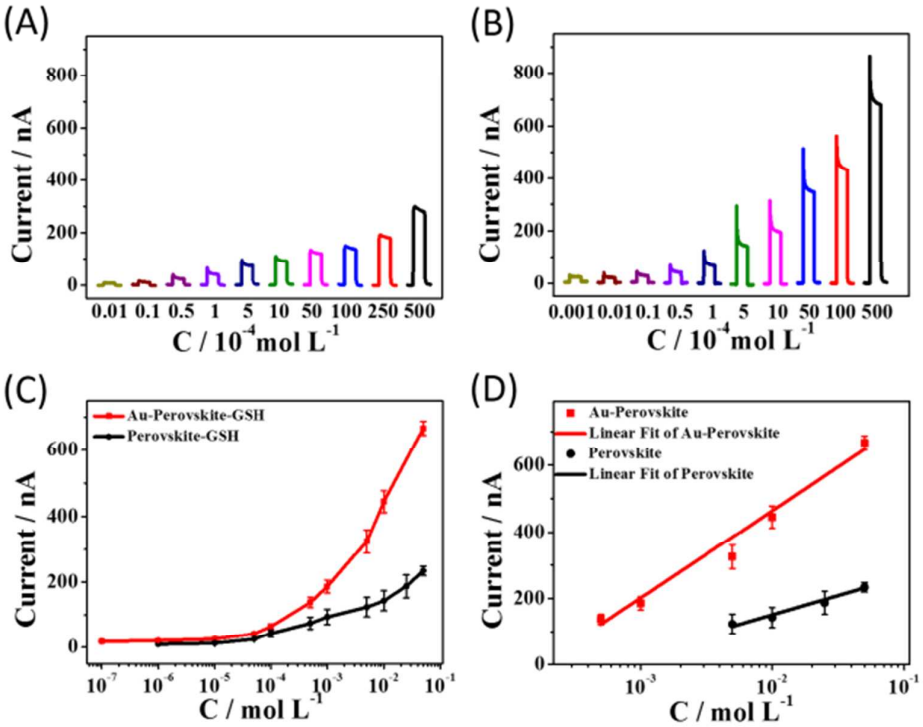

Figure S8. Photocurrents generated from (A) Bi_4NbO_8Cl and (B) Au NPs/Bi_4NbO_8Cl in 0.1 M PBS with variable GSH concentrations. (C) The specific working dependences, and (D) The corresponding linearity regions.

REFERENCES

1. Fujito, H.; Kunioku, H.; Kato, D.; Suzuki, H.; Higashi, M.; Kageyama, H.; Abe, R. *J. Am. Chem. Soc.* **2016**, *138*, 2082-2085.

2. Kuyper, A. C. *J. Am. Chem. Soc.* **1933**, *55*, 1722-1727.

3. Wu, X.; Thrall, E. S.; Liu, H.; Steigerwald, M.; Brus, L. *J. Phys. Chem. C* **2010**, *114*, 12896-12899.